JOURNAL OF COMPUTATIONAL PHYSICS 54, 260–277 (1984)

Guiding-Center Dispersion Function

P. SIMILON, J. E. SEDLAK, D. STOTLER,
H. L. BERK, W. HORTON, AND D. CHOI

Institute for Fusion Studies, University of Texas, Austin, Texas 78712

Received April 26, 1983

Analytic properties of the linear Vlasov response function for guiding-center particle motion in low frequency flute modes are investigated for a two-temperature Maxwell–Boltzmann plasma. Algorithms are given for evaluating the family of analytic functions $G_{m,n}(\omega)$ along with the software implementing the methods and user documentation on MFE files.

I. PLASMA PHYSICS ORIGIN OF GUIDING-CENTER DISPERSION FUNCTION (GCDF)

In this work we develop the properties of the family of special analytic functions that measure the linear response of the strongly magnetized, non-uniform collisionless plasma. The special functions occur in the conductivity tensor and charge density susceptibility required in theories of plasma waves, instabilities, and transport.

The typical problem in which the special functions occur is to find the response $\tilde{f}(\mathbf{x}, \mathbf{v}, t)$ in the particle distribution function to the electromagnetic perturbations $\tilde{\mathbf{E}}(\mathbf{x}) \exp(-i\omega t)$ and $\tilde{\mathbf{B}}(\mathbf{x}) \exp(-i\omega t)$ given the background equilibrium distribution function $F(\mathbf{x}, \mathbf{v})$. The equation for the response $\tilde{f}(\mathbf{x}, \mathbf{v}) \exp(-i\omega t)$ is

$$\left(-i\omega + \mathbf{v} \cdot \nabla + \frac{q}{mc} \mathbf{v} \times \mathbf{B}(\mathbf{x}) \cdot \frac{\partial}{\partial \mathbf{v}}\right) \tilde{f}(\mathbf{x}, \mathbf{v}) = -\frac{q}{m}\left(\tilde{\mathbf{E}} + \frac{\mathbf{v} \times \tilde{\mathbf{B}}}{c}\right) \cdot \frac{\partial F}{\partial \mathbf{v}}$$

where q and m are the mass and charge of the particles in the distribution $F(\mathbf{x}, \mathbf{v})$. The first order linear partial differential equation for $\tilde{f}(\mathbf{x}, \mathbf{v})$ is solved by integrating the source term on the right-hand side over the unperturbed particle trajectories $\dot{\mathbf{x}} = \mathbf{v}$ and $\dot{\mathbf{v}} = \mathbf{v} \times \Omega(\mathbf{x})$ where $\boldsymbol{\Omega} = q\mathbf{B}/mc$. The particle trajectories are the well-known helical cyclotron orbits with radius $\rho = v_\perp/\Omega$ and frequency Ω about the guiding-center drift velocity $\mathbf{v}_D$.

In general, the trajectories are

$$\mathbf{x}(t) = \mathbf{x}_0 + (v_\parallel \hat{b} + \mathbf{v}_D)t + \frac{v_\perp}{\Omega}\left[-\hat{e}_1 \sin(\zeta - \Omega t) + \hat{e}_2 \cos(\zeta - \Omega t)\right]$$

$$\mathbf{v}(t) = v_\parallel \hat{b} + \mathbf{v}_D + v_\perp[\hat{e}_1 \cos(\zeta - \Omega t) + \hat{e}_2 \sin(\zeta - \Omega t)]$$

0021-9991/84 $3.00

where the drift velocity is given by

$$\mathbf{v}_D = \frac{v_\perp^2 \hat{b} \times \nabla \ln B(\mathbf{x})}{2\Omega} + \frac{v_\parallel^2 \hat{b} \times (\hat{b} \cdot \nabla)\hat{b}}{\Omega}$$

with $\hat{b}(\mathbf{x}) = \mathbf{B}(\mathbf{x})/B(\mathbf{x})$ and $B(\mathbf{x}) = |\mathbf{B}(\mathbf{x})|$.

The complete theory of the inversion of the convective derivative for $\tilde{f}(\mathbf{x}, \mathbf{v})$ using the trajectories requires a complicated analysis whose details depend on the type of waves (high frequency $\omega \gg \Omega$ or low frequency $\omega \ll \Omega$) and the geometry (tokamak, mirror, or bumpy torus) of the system. The analysis, for example, is given in Ref. [1] for high frequency electrostatic modes and in Ref. [2] for low frequency electromagnetic modes.

1. Guiding-Center Propagator

For a particle of velocity $\mathbf{v}$ interacting with a fluctuation $\mathbf{k}\omega$ the linear response of the Vlasov equation is determined by the wave-particle propagator

$$g_{\mathbf{k}\omega}(\mathbf{v}) = \lim_{\varepsilon \to 0^+} \frac{1}{\omega - n\Omega - k_\parallel v_\parallel - \mathbf{k}_\perp \cdot \mathbf{v}_D + i\varepsilon}$$

where the limit $\varepsilon \to 0^+$ arises from the condition of causality in the response to the perturbation varying as $\exp(-i\omega t)$. The average response $R_{\mathbf{k}\omega}$ of the system to a velocity distribution of particles $F(\mathbf{v})$ is given by

$$R_{\mathbf{k}\omega} = \int d\mathbf{v}\, F(\mathbf{v})\, g_{\mathbf{k}\omega}(\mathbf{v}) = \langle g_{\mathbf{k}\omega}(\mathbf{v}) \rangle_F,$$

where $\int d\mathbf{v}\, F(\mathbf{v}) = 1$.

The special function measuring the response for $k_\parallel v_T \gg k_\perp v_D$ is the well-known Fried–Conte [3] plasma dispersion function

$$R^{F-C}_{k_\perp \omega} = \left\langle \frac{1}{\omega - k_\parallel v_\parallel + i0^+} \right\rangle_M = -\frac{1}{|k_\parallel| v_T} Z\left(\frac{\omega}{|k_\parallel| v_T}\right)$$

where $v_T = (2T/m)^{1/2}$ is the thermal velocity of the Maxwell–Boltzmann velocity distribution.

In general, for strongly magnetized plasmas, the most important perturbations for waves and instabilities have $k_\perp v_D \gg k_\parallel v_T$. Such perturbations and waves are called flute modes ($k_\parallel = 0$) and flute-like modes ($k_\parallel v_T \ll k_\perp v_D$) and are of special importance in the dynamics of plasmas. This fact leads to the definition of the guiding-center response function [4]

$$R^{GCDF}_{k_\perp, \omega} = \left\langle \frac{1}{\omega - k_\perp v_D + i0^+} \right\rangle_M$$

and the homogeneous function $G(\omega) = \omega R_{k_\perp,\omega}$ whose properties are developed in Sections II and III.

2. Two-Temperature Maxwell-Boltzmann Average

Recent studies of plasmas containing hot electron components such as the bumpy torus and tandem mirror end cell plasmas require the guiding-center dispersion for highly anisotropic velocity distributions [5]. To take into account the anisotropy the dimensionless drift frequencies ω_g and ω_c are defined by

$$\omega_D = \omega_g \frac{mv_\perp^2}{2T_\perp} + \omega_c \frac{mv_\parallel^2}{T_\parallel}$$

where

$$\omega_g = \mathbf{k} \cdot \frac{cT_\perp}{eB} \frac{\hat{b} \times \nabla B}{B}$$

$$\omega_c = \mathbf{k} \cdot \frac{cT_\parallel}{eB} \hat{b} \times (\hat{b} \cdot \nabla)\hat{b}$$

where $T_\perp = \langle \frac{1}{2} mv_\perp^2 \rangle$ and $T_\parallel = \langle mv_\parallel^2 \rangle$. The simple response function for the two-temperature Maxwell–Boltzmann velocity distribution $F_M(v_\perp, v_\parallel)$ is then

$$R_{k_\perp \omega}^{GC} = \frac{1}{\pi^{1/2}} \int_0^\infty dx \int_0^\infty dy\, y^{-1/2} \frac{e^{-x-y}}{\omega - \omega_g x - 2\omega_c y}$$

for $\mathrm{Im}(\omega) > 0$.

Taking into account the finite-Larmor radius (FLR) effects gives the generalized response function

$$\int \frac{(mv_\perp^2/2T_\perp)^{m-1}(mv_\parallel^2/2T_\parallel)^{n-1} J_0^2(k_\perp v_\perp/\Omega)}{\omega - \omega_g(mv_\perp^2/2T_\perp) - \omega_c(mv_\parallel^2/T_\parallel)} F_M(v_\perp, v_\parallel)\, d\mathbf{v}$$

$$= \frac{1}{\pi^{1/2}} \int_0^\infty dx \int_0^\infty dy\, y^{-1/2} \exp(-x-y) \frac{x^{m-1} y^{n-1} J_0^2(k\sqrt{2x})}{\omega - \omega_g x - 2\omega_c y}$$

where $k = k_\perp (T_\perp/m)^{1/2}/\Omega$. The further generalizations required for the electromagnetic 3×3 dispersion relation are given in Section IV(7).

For $m = n = 1$ the primary FLR response function is defined by

$$G^{FLR}(\omega, a, b, k) \equiv \frac{\omega}{\pi^{1/2}} \int_0^\infty dx \int_0^\infty dy\, y^{-1/2} \exp(-x-y) \frac{J_0^2(k\sqrt{2x})}{\omega - ax - by}.$$

For small k the FLR velocity space moments may be expanded in powers of $(k^2x)^l$ and expressed in terms of $G_{m+l,n}(\omega)$, defined below.

The primary response function $G(\omega, a, b) = G_{1,1}$ is related to the Maxwell–Boltzmann averaged propagator by

$$\frac{\omega}{\pi^{1/2}} \int_0^\infty dx \int_0^\infty dy \frac{y^{-1/2} \exp(-x-y)}{\omega - \omega_g x - 2\omega_c y}$$

$$= \int_0^\infty u\, du \exp(-u^2/2) \int_{-\infty}^\infty \frac{dv \exp(-v^2/2)}{(2\pi)^{1/2}} \frac{\omega}{\omega - \frac{1}{2}\omega_g u^2 - \omega_c v^2}$$

$$= G_{1,1}(\omega, \omega_g, 2\omega_c) \equiv G(\omega, \omega_g, 2\omega_c).$$

The generalized dispersion function is related to the Maxwell–Boltzmann average by

$$\int_0^\infty u\, du \exp(-u^2/2) \int_{-\infty}^\infty dv \frac{\exp(-v^2/2)}{(2\pi)^{1/2}} \frac{\omega}{\omega - \frac{1}{2}\omega_g u^2 - \omega_c v^2} (u^2/2)^{m-1} (v^2/2)^{n-1}$$

$$= D_{m,n} G_{m,n}(\omega, \omega_g, 2\omega_c) \qquad \text{for} \quad \mathrm{Im}(\omega) > 0$$

where

$$D_{m,n} \equiv \frac{\Gamma(m)\,\Gamma(n-\frac{1}{2})}{\Gamma(\frac{1}{2})} \qquad \text{with} \quad D_{1,1} = 1.$$

II. Mathematical Properties of the Guiding-Center Dispersion Function

1. *Definitions and Properties*

1.1 *Definition*

The generalized guiding-center dispersion function $G_{m,n}(\omega, a, b)$ is defined for real a, b, integer m, n, and complex ω by

$$G_{m,n}(\omega, a, b) \equiv -i\omega \int_0^\infty dt \exp[i\omega t](1 + iat)^{-m}(1 + ibt)^{-n+1/2} \qquad (1.1.1)$$

for $\mathrm{Im}(\omega) > 0$, and the analytic continuation for other ω. The determination of $(1 + ibt)^{1/2}$ is chosen such that its real part is positive. The function $G_{m,n}(\omega, a, b)$ has a branch point at $\omega = 0$ with the branch line taken from $\omega = 0$ to $-i\infty$.

1.2. *Primary Response Function*

The fundamental guiding-center response function $G(\omega, a, b)$ occurs for $m = n = 1$:

$$G(\omega, a, b) \equiv G_{1,1}(\omega, a, b). \qquad (1.2.1)$$

1.3. *Alternate Integral Formula*

$$G_{m,n}(\omega, a, b) = \int_0^\infty ds\, e^{-s} \left(1 - \frac{as}{\omega}\right)^{-m} \left(1 - \frac{bs}{\omega}\right)^{-n+1/2} \tag{1.3.1}$$

for $\mathrm{Im}(\omega) > 0$ and $\mathrm{Re}(1 - bs/\omega)^{1/2} > 0$.

1.4. *Homogeneity, Symmetry, and Large ω Limit*

Homogeneity. If r is real and positive, $r > 0$, then

$$G_{m,n}(r\omega, ra, rb) = G_{m,n}(\omega, a, \mathrm{b}). \tag{1.4.1}$$

Symmetry. For all ω

$$G_{m,n}(-\omega^*, -a, -b) = G^*_{m,n}(\omega, a, b). \tag{1.4.2}$$

Limit for Large $|\omega|$. For a and b fixed and $|\omega| \to \infty$

$$G_{m,n}(\omega, a, b) \to 1, \qquad \text{if} \quad \arg \omega \neq -\pi/2 \ (\mathrm{mod}\ 2\pi). \tag{1.4.3}$$

2. *Recursion Relations and Differential Properties*

$$a \frac{\partial G_{m,n}(\omega, a, b)}{\partial \omega} = \left(\frac{a}{\omega} - 1\right) G_{m,n}(\omega, a, b) + G_{m-1,n}(\omega, a, b) \tag{2.1}$$

$$b \frac{\partial G_{m,n}(\omega, a, b)}{\partial \omega} = \left(\frac{b}{\omega} - 1\right) G_{m,n}(\omega, a, b) + G_{m,n-1}(\omega, a, b) \tag{2.2}$$

$$(a - b)\, G_{m,n}(\omega, a, b) = aG_{m,n-1}(\omega, a, b) - bG_{m-1,n}(\omega, a, b) \tag{2.3}$$

$$G_{m,n} = 1 + \frac{ma}{\omega} G_{m+1,n} + \left(n - \frac{1}{2}\right) \frac{b}{\omega} G_{m,n+1} \tag{2.4}$$

$$G_{m,n} = 1 + \left(m + n - \frac{1}{2}\right) \frac{a}{\omega} G_{m+1,n} - \left(n - \frac{1}{2}\right) \frac{(a-b)}{\omega} G_{m+1,n+1} \tag{2.5}$$

$$G_{m,n} = 1 + \left(m + n - \frac{1}{2}\right) \frac{b}{\omega} G_{m,n+1} + \frac{m(a-b)}{\omega} G_{m+1,n+1} \tag{2.6}$$

$$G_{0,0}(\omega, a, b) = 1 - \frac{b}{2\omega} G_{0,1}(\omega, a, b) \tag{2.7}$$

$$\frac{\partial G_{m,n}(\omega, a, b)}{\partial a} = -\frac{m}{a} G_{m,n}(\omega, a, b) + \frac{m}{a} G_{m+1,n}(\omega, a, b) \tag{2.8}$$

$$\frac{\partial G_{m,n}(\omega, a, b)}{\partial b} = -\frac{n - \frac{1}{2}}{b} G_{m,n}(\omega, a, b) + \frac{n - \frac{1}{2}}{b} G_{m,n+1}(\omega, a, b) \tag{2.9}$$

$$a\frac{\partial G_{m,n}(\omega, a, b)}{\partial a} + b\frac{\partial G_{m,n}(\omega, a, b)}{\partial b} + \omega\frac{\partial G_{m,n}(\omega, a, b)}{\partial \omega} = 0. \tag{2.10}$$

3. *Analytic Continuation for* $\mathrm{Im}(\omega) \leqslant 0$

$G_{m,n}(\omega, a, b)$ is analytic for $\mathrm{Im}(\omega) > 0$, but when extended into $\mathrm{Im}(\omega) \leqslant 0$ it is necessary to introduce the branch cut from $\omega = 0$. The cut can be arbitrarily placed in the $\mathrm{Im}(\omega) < 0$ plane. Unless otherwise specified we define the cut by $\omega_b = -it$ with $0 \leqslant t \leqslant \infty$.

3.1. *Analytic Continuation from Integral Representation*

For integral representation (1.3.1) the analytic continuation is given by the contour integral

$$G_{m,n}(\omega, a, b) = \int_C ds\, e^{-s} \left(1 - \frac{as}{\omega}\right)^{-m} \left(1 - \frac{bs}{\omega}\right)^{-n+1/2} \tag{3.1.1}$$

with the contour C going, if necessary, below the singular point $s_1 = \omega/a$ and branch point $s_2 = \omega/b$ from $s = 0$ to $s = +\infty$ as shown in Fig. 1.

3.2. *Analytic Continuation from Differential Equation*

The differential relations (2.1), (2.2), and (2.7) are a closed set of differential equations of the Fuchsian type with $\omega = 0$ a regular singular point.

Analytic continuation and computations are made using the definition (1.3.1) for initial data ω_0 with $\mathrm{Im}(\omega_0) > 0$ and integrating (2.1), (2.2), and (2.7) to ω with $\mathrm{Im}(\omega) < 0$, along path P shown in Fig. 2.

For example, the value of $G(\omega, a, b)$ is found from

$$y_1 = G_{1,1}(\omega, a, b) \tag{3.2.1}$$

$$y_2 = G_{0,1}(\omega, a, b) \tag{3.2.2}$$

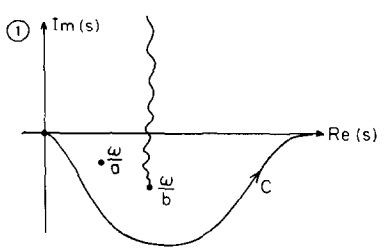

FIG. 1. Integration contour C (Section II(3.1)).

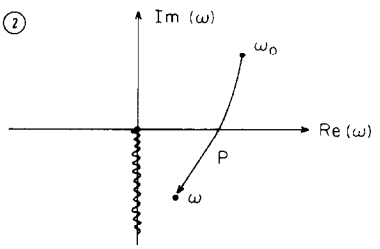

FIG. 2. Path P (Section II(3.2)).

$$\frac{dy_1}{d\omega} = \left(\frac{1}{\omega} - \frac{1}{a}\right) y_1 + \frac{1}{a} y_2 \tag{3.2.3}$$

$$\frac{dy_2}{d\omega} = \left(\frac{1}{2\omega} - \frac{1}{b}\right) y_2 + \frac{1}{b} \tag{3.2.4}$$

with initial data $\omega_0 = \omega + i\sigma$ evaluated using the integral (1.3.1) definition.

4. *Integral Solutions of Differential Equations*

4.1. *Definitions of $K_1(a, b)$ and $K_2(a, b)$*

For $a \neq 0$, $b \neq 0$ and complex ω (with positive or negative imaginary parts) the solutions of (3.2.3) and (3.2.4) are

$$\begin{aligned} y_1(\omega) = {} & \frac{2\omega^2}{ab} \exp\left(-\frac{\omega}{a}\right) \int_0^1 dt \, \frac{\exp[\sigma(t)] - 1}{\sigma(t)} \\ & + 2K_1 \frac{\omega}{a} \omega^{1/2} \exp\left(-\frac{\omega}{a}\right) \int_0^1 \exp\left[\left(\frac{\omega}{a} - \frac{\omega}{b}\right) t^2\right] dt \\ & + \omega K_2 \exp\left(-\frac{\omega}{a}\right) \end{aligned} \tag{4.11}$$

$$y_2(\omega) = \frac{2\omega}{b} \exp\left(-\frac{\omega}{b}\right) \int_0^1 dt \exp\left(\frac{\omega}{b} t^2\right) + K_1 \omega^{1/2} \exp\left(-\frac{\omega}{b}\right) \tag{4.1.2}$$

where

$$\sigma(t) \equiv \frac{\omega}{a} - \frac{\omega}{b} + \frac{\omega}{b} t^2 \tag{4.1.3}$$

and $(e^\sigma - 1)/\sigma$ is analytic in t. The constants K_1 and K_2 are determined by identifying the asymptotic behavior of $y_1(\omega)$ and $y_2(\omega)$ with the integral representation of $G_{1,1}$ and $G_{0,1}$, for $\omega \to 0$:

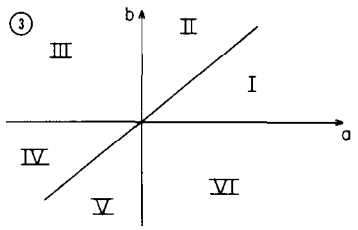

FIG. 3. Regions in the (a, b) parameter space (Section II(4.1)).

$$y_1(\omega) \sim K_2 \omega \tag{4.1.4}$$

$$y_2(\omega) \sim K_1 \omega^{1/2}. \tag{4.1.5}$$

The values of K_1 and K_2 are given for the regions I–VI of the a–b plane defined in Fig. 3.

DEFINITION OF $K_1(a, b)$

$b > 0$, Regions I, II, III

$$K_1 = -i(\pi/b)^{1/2}. \tag{4.1.6}$$

$b < 0$, Regions IV, V, VI

$$K_1 = (\pi/|b|)^{1/2}. \tag{4.1.7}$$

DEFINITION OF $K_2(a, b)$

$1 > b/a > 0$, Regions I, IV

$$K_2 = \frac{1}{a(1 - b/a)^{1/2}} \ln \frac{1 - (1 - b/a)^{1/2}}{1 + (1 - b/a)^{1/2}} \tag{4.1.8}$$

$b/a > 1$, Regions II, V

$$K_2 = -\frac{2 \arctan(b/a - 1)^{1/2}}{a(b/a - 1)^{1/2}} \tag{4.1.9}$$

$b/a < 0$, Regions III, VI

$$K_2 = \frac{1}{(1 + |b/a|)^{1/2}} - \left[i \frac{\pi}{|a|} + \frac{1}{a} \ln \frac{(1 + |b/a|)^{1/2} - 1}{(1 + |b/a|)^{1/2} + 1} \right] \tag{4.1.10}$$

$b = a$,

$$K_2 = -2/a. \tag{4.1.11}$$

4.2. *Small-Argument Limit*

For $|\omega| \ll |a|, |b|$ the integral solutions of the differential equations give the small-argument expansions

$$G(\omega, a, b) \sim K_2(a, b)\left[\omega - \frac{\omega^2}{a} + \frac{\omega^3}{2a^2} + \cdots\right] + K_1(a, b)\left[\frac{2}{a}\omega^{3/2} - \frac{2}{3a}\left(\frac{1}{b} + \frac{2}{a}\right)\omega^{5/2} + \cdots\right] + \frac{2}{ab}\omega^2 - \frac{1}{ab}\left(\frac{2}{3b} + \frac{1}{a}\right)\omega^3 + \cdots + O(\omega^{7/2}) \tag{4.2.1}$$

$$G_{0,1}(\omega, a, b) \sim K_1(a, b)\left[\omega^{1/2} - \frac{1}{b}\omega^{3/2} + \frac{1}{2b^2}\omega^{5/2} + \cdots\right] + \left[\frac{2}{b}\omega - \frac{4}{3}\frac{\omega^2}{b^2} + \frac{8}{15}\frac{\omega^3}{b^3} + \cdots\right] + O(\omega^{7/2}). \tag{4.2.2}$$

4.3. *Imaginary Part of $G(\omega, a, b)$ for real ω*

Assume real, positive ω. For real $\omega < 0$ use the symmetry $G(-\omega, a, b) = G^*(\omega, -a, -b)$, Eq. (1.4.2). One has

$$\operatorname{Im} G(\omega, a, b) = -\pi(2\pi)^{-1/2}\int_{-\infty}^{+\infty} dv \exp(-v^2/2)\int_0^{\infty} u\, du \exp(-u^2/2) \times \delta\left(1 - \frac{bv^2}{2\omega} - \frac{au^2}{2\omega}\right). \tag{4.3.1}$$

where $\delta(x)$ is the Dirac delta function.
The Im $G(\omega, a, b)$ occurs from the resonance on the ellipse or hyperbola in the u, v plane.

$$\operatorname{Im} G(\omega, a, b) = -(2\pi)^{1/2}\frac{\omega}{|a|}\exp\left(-\frac{\omega}{a}\right) \times \int_0^{\infty} dv \exp(-v^2(a-b)/2a)\, H\left(\frac{\omega - bv^2/2}{a}\right) \tag{4.3.2}$$

where $H(x)$ is the Heaviside step function.

$a > 0,\ b > 0$; Regions I, II

$$\operatorname{Im} G(\omega, a, b) = -(2\pi)^{1/2} \frac{\omega}{a} \exp\left(-\frac{\omega}{a}\right)\left(\frac{2\omega}{b}\right)^{1/2} \int_0^1 dt \times \exp\left(\frac{\omega(b-a)}{ab} t^2\right) \tag{4.3.3}$$

$a > 0,\ b < 0$; Region VI

$$\operatorname{Im} G(\omega, a, b) = -\pi \left(\frac{\omega}{a}\right) \exp\left(-\frac{\omega}{a}\right)\left(\frac{a}{a+|b|}\right)^{1/2} \tag{4.3.4}$$

$a < 0,\ b > 0$; Region III

$$\operatorname{Im} G(\omega, a, b) = -(2\pi)^{1/2} \frac{\omega}{|a|} \exp\left(\frac{\omega}{|a|}\right)\left(\frac{2\omega}{b}\right)^{1/2} \int_1^\infty dt \times \exp\left(-\frac{\omega(|a|+b)}{|a|\, b} t^2\right) \tag{4.3.5}$$

$a \leqslant 0,\ b \leqslant 0$; Regions IV, V

$$\operatorname{Im} G(\omega, a, b) = 0 \tag{4.3.6}$$

$a = 0,\ b > 0$;

$$\operatorname{Im} G(\omega, a, b) = -\pi^{1/2} \left(\frac{\omega}{b}\right)^{1/2} \exp\left(-\frac{\omega}{b}\right) \tag{4.3.7}$$

$b = 0,\ a > 0$;

$$\operatorname{Im} G(\omega, a, b) = -2\pi \frac{\omega}{a} \exp\left(-\frac{\omega}{a}\right). \tag{4.3.8}$$

5. *Relations between the Function Values in the Upper and Lower ω Half-Plane*

If $\operatorname{Im}(\omega) > 0$ and $\omega = re^{i\theta}$ with $0 < \theta < \pi$, so that $\omega^* = re^{-i\theta}$ and $\omega^{1/2} = r^{1/2} e^{i\theta/2}$, then from the solutions of the equations we obtain

$$G^*_{0,1}(\omega^*, a, b) - G_{0,1}(\omega, a, b) = -2\omega^{1/2} \exp\left(-\frac{\omega}{b}\right) \times \begin{cases} \operatorname{Re} K_1 & \text{if } \theta > \pi/2 \\ i \operatorname{Im} K_1 & \text{if } \theta < \pi/2 \end{cases} \tag{5.1}$$

$$G^*_{1,1}(\omega^*, a, b) - G_{1,1}(\omega, a, b)$$
$$= -2i\omega \exp\left(-\frac{\omega}{a}\right) \times \operatorname{Im} K_2 - 4\frac{\omega}{a}\omega^{1/2} \exp\left(-\frac{\omega}{a}\right)$$
$$\times \int_0^1 dt \exp\left[\left(\frac{\omega}{a} - \frac{\omega}{b}\right) t^2\right] \times \begin{cases} \operatorname{Re} K_1 & \text{if } \theta > \pi/2 \\ i \operatorname{Im} K_1 & \text{if } \theta < \pi/2 \end{cases} \tag{5.2}$$

with the values of $K_1(a, b)$ and $K_2(a, b)$ given in Section 4.1.

6. *Asymptotic Behavior*

For the fluid limit $|\omega| \gg |a|, |b|$, and $\arg(\omega) \neq -\pi/2$.

$$G_{m,n}(\omega, a, b) \sim \sum_{j=0}^{\infty} \frac{j!}{\omega^j} \sum_{l=0}^{j} \binom{-m}{j-l} \binom{-n+1/2}{l} (-a)^{j-l}(-b)^l$$
$$\sim 1 + \frac{1}{\omega}\left[ma + \left(n - \frac{1}{2}\right) b\right]$$
$$+ \frac{2}{\omega^2}\left[\frac{m(m+1)}{2} a^2 + m\left(n - \frac{1}{2}\right) ab + \frac{1}{2}\left(n - \frac{1}{2}\right)\left(n + \frac{1}{2}\right) b^2\right]$$
$$+ \cdots \tag{6.1}$$

$$G_{1,1}(\omega, a, b) \sim \sum_{j=0}^{\infty} \frac{j!}{\omega^j} \sum_{l=0}^{j} \binom{-1/2}{l} a^{j-l}(-b)^l$$
$$\sim 1 + \frac{1}{\omega}\left(a + \frac{1}{2} b\right) + \frac{2}{\omega^2}\left(a^2 + \frac{1}{2} ab + \frac{3}{8} b^2\right) + \cdots \tag{6.2}$$

$$G_{0,1}(\omega, a, b) \sim \sum_{j=0}^{\infty} \frac{j!}{\omega^j} \binom{-1/2}{j} (-b)^j$$
$$\sim 1 + \frac{b}{2\omega} + \frac{3}{4}\frac{b^2}{\omega^2} + \cdots \tag{6.3}$$

where $\binom{z}{j}$ is the usual binomial coefficient.

7. *Integral Representation of the FLR Dispersion Functions*

The integral representation for the FLR dispersion function $G^{\mathrm{FLR}}(\omega, a, b, k)$ defined in Section I(2),

$$G^{\mathrm{FLR}}(\omega, a, b, k) = \int_0^{\infty} u\, du \exp(-u^2/2) \int_{-\infty}^{+\infty} dv \frac{\exp(-v^2/2)}{(2\pi)^{1/2}}$$
$$\times \frac{\omega J_0^2(ku)}{\omega - \frac{1}{2}au^2 - \frac{1}{2}bv^2} \tag{7.1}$$

where $k = k_\perp (T_\perp/m)^{1/2}/\Omega$, is

$$G^{\mathrm{FLR}}(\omega, a, b, k) = -i\omega \int_0^\infty \frac{dt \exp(i\omega t)\, \Gamma_0[k^2/(1+iat)]}{(1+iat)(1+ibt)^{1/2}} \tag{7.2}$$

$$= \int_C ds \frac{e^{-s}\Gamma_0[k^2/(1-as/\omega)]}{(1-as/\omega)(1-bs/\omega)^{1/2}} \tag{7.3}$$

where $\Gamma_0(z) = e^{-z}I_0(z) = \pi^{-1}\int_0^\pi d\theta \exp[-z(1-\cos\theta)]$ and C is the contour defined in Fig. 1. Note that Γ_0 has an essential singularity at $s = \omega/a$.

A set of finite-Larmor radius dispersion functions is defined as

$$G_i^{\mathrm{FLR}}(\omega, a, b, k) = \frac{\omega}{\sqrt{\pi}} \int_0^\infty dx \int_0^\infty dy\, y^{-1/2} \frac{\exp(-x-y)}{\omega - ax - by} F_i(x, y, k) \tag{7.4}$$

where we take

$$F_i(x, y, k) = \begin{bmatrix} J_0^2(kq), & i=1 \\ J_1^2(kq), & i=2 \\ \dfrac{q}{k} J_0(kq) J_1(kq), & i=3 \\ (x+y) J_0^2(kq), & i=4 \\ (x+y) J_1^2(kq), & i=5 \\ (x+y)\dfrac{q}{k} J_0(kq) J_1(kq), & i=6 \end{bmatrix} \tag{7.5}$$

with $q = (2x)^{1/2}$. The first function, G_1^{FLR}, is the G^{FLR} in Eq. (7.1). The integral representations for G_i^{FLR} are obtained from Eq. (7.3). For example, the representation for G_2^{FLR} is obtained from (7.3) by replacing $\Gamma_0(z)$ by $\Gamma_1(z) = e^{-z}I_1(z)$, where $I_1(z)$ is the modified Bessel function.

From Eq. (7.5) we see that

$$G_3^{\mathrm{FLR}} = -\frac{1}{2k}\frac{\partial}{\partial k} G_1^{\mathrm{FLR}} \tag{7.6}$$

and

$$G_6^{\mathrm{FLR}} = -\frac{1}{2k}\frac{\partial}{\partial k} G_4^{\mathrm{FLR}}. \tag{7.7}$$

With Eq. (7.6) we immediately obtain the integral representation

$$G_3^{\mathrm{FLR}} = \int_C \frac{ds\, e^{-s}[\Gamma_0(z) - \Gamma_1(z)]}{(1-as/\omega)^2(1-bs/\omega)^{1/2}} \tag{7.8}$$

with $z = k^2/(1-as/\omega)$.

For G_4^{FLR}, if we write $(x+y)$ in Eq. (7.5) as

$$x+y=[\omega-(\omega-ax-by)+(a-b)y]/a, \tag{7.9}$$

then the integral separates into three terms,

$$\begin{aligned} G_4^{\mathrm{FLR}} &= \frac{\omega}{a}\left[G_1^{\mathrm{FLR}}-\Gamma_0(k^2)\right] \\ &\quad + \frac{a-b}{a}\frac{\omega}{\sqrt{\pi}}\int_0^\infty dx\int_0^\infty dy\, y^{1/2}\,\frac{\exp(-x-y)\,J_0^2(k\sqrt{2x})}{\omega-ax-by} \\ &= \frac{\omega}{a}\left[G_1^{\mathrm{FLR}}-\Gamma_0(k^2)\right]+\frac{a-b}{2a}\int_C \frac{ds\,e^{-s}\Gamma_0(z)}{\left(1-\dfrac{as}{\omega}\right)\left(1-\dfrac{bs}{\omega}\right)^{3/2}}, \end{aligned} \tag{7.10}$$

again with $z=k^2/(1-as/\omega)$. Similarly, we have

$$\begin{aligned} G_5^{\mathrm{FLR}} &= \frac{\omega}{a}\left[G_2^{\mathrm{FLR}}-\Gamma_1(k^2)\right] \\ &\quad + \frac{a-b}{2a}\int_C \frac{ds\,e^{-s}\Gamma_1(z)}{(1-as/\omega)(1-bs/\omega)^{3/2}}. \end{aligned} \tag{7.11}$$

We obtain the representation of the sixth FLR dispersion function from Eq. (7.7),

$$\begin{aligned} G_6^{\mathrm{FLR}} &= \frac{\omega}{a}\left[G_3^{\mathrm{FLR}}-\Gamma_0(k^2)+\Gamma_1(k^2)\right] \\ &\quad + \frac{a-b}{2a}\int_C \frac{ds\,e^{-s}[\Gamma_0(z)-\Gamma_1(z)]}{(1-as/\omega)^2(1-bs/\omega)^{3/2}}. \end{aligned} \tag{7.12}$$

When $\mathrm{Im}(\omega)>0$, the integration contour for these functions can be taken along the real axis from zero to infinity. If ω is in the lower half-plane, the contour must be deformed to remain below the singularities.

Alernatively, these functions may be generated by expanding Γ_0 and $\Gamma_1(k^2/(1-as/\omega))$. This yields a power series in k^2 with coefficients related to the non-FLR guiding-center functions $G_{m,1}$ and $G_{m,2}$. Thus,

$$G_1^{\mathrm{FLR}}=\sum_{j=0}^{\infty}(k^2)^{2j}\,c_j G_{2j+1,1}-\sum_{j=0}^{\infty}(k^2)^{2j+1}d_j G_{2j+2,1} \tag{7.13}$$

$$\begin{aligned} G_4^{\mathrm{FLR}} &= \frac{\omega}{a}\left[G_1^{\mathrm{FLR}}-\Gamma_0(k^2)\right] \\ &\quad + \frac{a-b}{2a}\left[\sum_{j=0}^{\infty}(k^2)^{2j}\,c_j G_{2j+1,2}-\sum_{j=0}^{\infty}(k^2)^{2j+1}d_j G_{2j+2,2}\right] \end{aligned} \tag{7.14}$$

where

$$c_j = \sum_{i=0}^{j} \frac{1}{4^i (i!)^2 (2j-2i)!} \tag{7.15}$$

$$d_j = \sum_{i=0}^{j} \frac{1}{4^i (i!)^2 (2j-2i+1)!}. \tag{7.16}$$

The $G_{m,n}$ may be obtained using the algorithm described in Section III(1) and the recursion relations (2.3)–(2.6). With ω, a, and b of order unity, and $k < 1.5$, the sums (7.13)–(7.14) converge to a part in 10^4 after 30 or fewer terms ($j \leqslant 14$). With larger k, one is limited by the loss of precision in $G_{m,n}$ for large m.

III. Numerical Algorithms for the Guiding-Center Dispersion Function

1. *Evaluaton of $G_{m,n}(\omega, a, b)$ from Integral and Differential Representations*

A FORTRAN function subprogram, GCDF, has been written to generate the first none guiding-center dispersion functions, $G_{m,n}(\omega, a, b)$, for m and n running from 0 to 2. The functions are evaluated either from the integral formula, Eq. (1.3.1), or from the differential representation, Eqs. (2.1), (2.2), (2.7). The choice depends on the complex frequency ω. First, for ω nonzero, the parameters ω, a, and b are transformed using the homogeneity property (1.4.1),

$$(\omega, a, b) \rightarrow (\omega/r, a/r, b/r)$$

$$r = \mathrm{Abs}(\omega)$$

so that ω lies on the unit circle. In the following discussion, ω, a, and b refer to these rescaled values.

It should be noted that if a, b, and $(a-b)$ are nonzero then all the $G_{m,n}$, for arbitrary m and n, can be obtained from $G_{0,1}$ and $G_{1,1}$ using the recursion relations (2.3)–(2.7). However, these relations include terms such as $(G_{m+1,n} - G_{m,n})/a$. When parameter a is near zero the dominant part of $G_{m+1,n} - G_{m,n}$ is linear in a/ω, and serious numerical errors will result from the finite precision arithmetic. Various small-a expansions can be derived for such cases, but these are not satisfactory if ω happens to be near the negative imaginary axis. There, low-order expansions cannot reproduce the term $\exp(-\omega/a)$ in Eq. (4.1.1). Similar errors occur when b or $(a-b)$

is near zero. For these reasons the recursion relations have been avoided in the GCDF subprogram; all the $G_{m,n}$ (except $G_{0,0}$) are obtained by integrating Eq. (1.3.1) or Eqs. (2.1) and (2.2).

There are singularities in the integrand of Eq. (1.3.1) at $s_1 = \omega/a$ and $s_2 = \omega/b$. If the real parts of both s_1 and s_2 are negative then this integral correctly gives the guiding-center functions for any Imag(ω). If either s_1 or s_2 has a positive real part then Eq. (1.3.1) applies only if Imag(ω) is positive. In the latter case the program uses this integral representation only when Imag(ω) > 0.4. This pushes the singular points away from the real axis, making it easier to obtain a numerical solution. The set of subroutines, GCINIT, GCSIMP, and GINTGR, performs the integrations by the Simpson method on all the $G_{m,n}$ simultaneously. GCINIT divides the range of integration into six subintervals. If parameter a or b is large, one of the singularities will be close to the origin. The widths of the first two subintervals then are taken inversely proportional to $|a|$ or $|b|$ to cover the region where the integrand varies fastest.

In all other cases, Imag(ω) $\leqslant$ 0.4 and Real(s_1) or Real(s_2) positive, the system of differential equations (2.1), (2.2), (2.7) must be solved. The initial conditions are established at the point $\omega_0 = (\text{Real}(\omega), 0.5)$, calling GCINIT to evaluate the $G_{m,n}(\omega_0)$.

The differential system is approximated by the implicit finite-difference equations

$$G_{0,1}^{(i+1)} - G_{0,1}^{(i)} = \left[\frac{1}{2\omega} G_{0,1}^{(i)} - \frac{1}{b} G_{0,1}^{(i+1)} + \frac{1}{b}\right] d\omega$$

$$G_{1,1}^{(i+1)} - G_{1,1}^{(i)} = \left[\frac{1}{\omega} G_{1,1}^{(i)} - \frac{1}{a} G_{1,1}^{(i+1)} + \frac{1}{a} G_{0,1}^{(i+1)}\right] d\omega$$

and similar expressions for the other $G_{m,n}$. Rearranging terms yields

$$G_{0,1}^{(i+1)} = G_{0,1}^{(i)} \frac{b}{b + d\omega}\left(1 + \frac{d\omega}{2\omega}\right) + \frac{d\omega}{b + d\omega}$$

$$G_{1,1}^{(i+1)} = G_{1,1}^{(i)} \frac{a}{a + d\omega}\left(1 + \frac{d\omega}{\omega}\right) + G_{0,1}^{(i+1)} \frac{d\omega}{a + d\omega}.$$

The integration contour is taken to be the straight line from ω_0 to ω so that $d\omega$ is purely imaginary. Then the factors $a/(a + d\omega)$ and $b/(b + d\omega)$ have magnitude less than one for all real a and b. With this choice the algorithm is stable if $d\omega/\omega$ is small everywhere on the contour. This requires $|d\omega| \ll |\text{Real}(\omega)|$.

It can be shown that if a and b approach zero with $d\omega$ held fixed, the above expressions go to the correct asymptotic limits as given in Section II(6). Thus, the step size can be chosen independently of a and b as long as $|\text{Real}(\omega)|$ is not too small (ω not too near the branch cut).

2. *Software Documentation*

The FORTRAN code for the guiding-center dispersion function is available on the MFE network. It may be copied from FILEM, user number 014545, file GCDFIFS. This file contains the complex function GCDF and its subroutines GCINIT, GCSIMP, and GINTGR. Documentation and an example also are included.

3. *Graphs of* $G(\omega, a, b)$ *versus* Real(ω) *for Various* a, b, *and* Imag(ω)

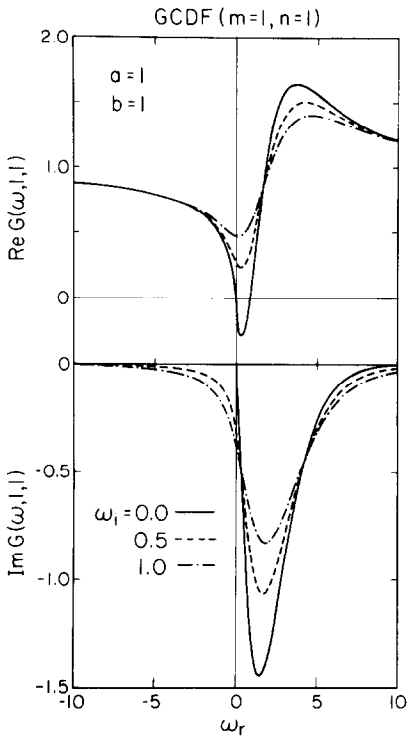

FIG. 4. Graph of the real and imaginary parts of $G(\omega, a, b)$ as a function of $\omega_r = \text{Real}(\omega)$ for $a = b = 1$ and $\omega_i = \text{Imag}(\omega) = 0.$, 0.5, and 1.0.

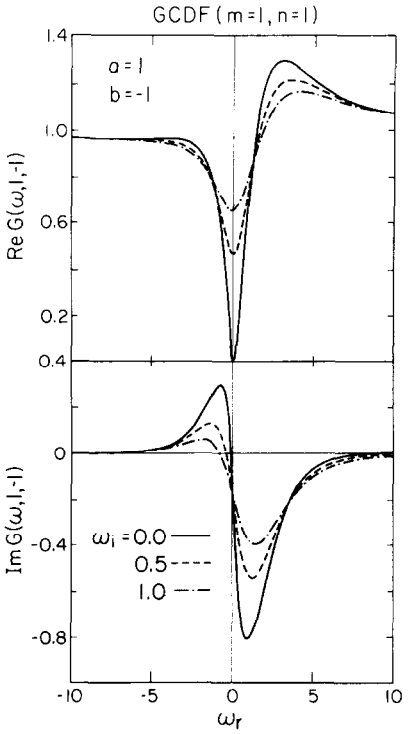

FIG. 5. Graph of the real and imaginary parts of $G(\omega, a, b)$ as a function of $\omega_r = \text{Real}(\omega)$ for $a = 1$ and $b = -1$ with $\omega_i = 0.$, 0.5, and 1.0.

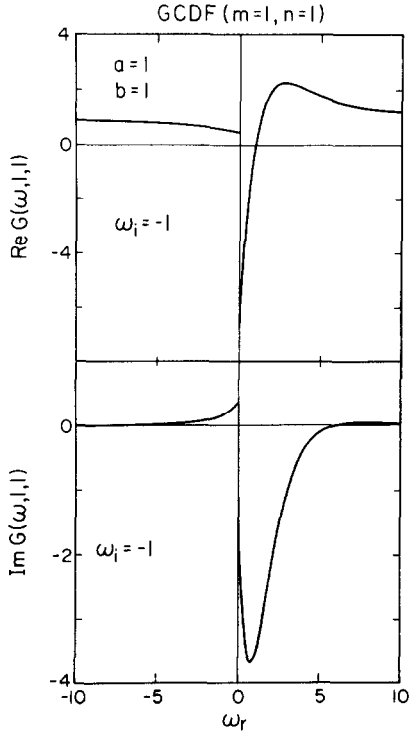

FIG. 6. Graph of the real and imaginary parts of $G(\omega, a = 1, b = 1)$ for $\omega_i = -1$. The discontinuity at $\omega_r = 0$ arises from the branch line shown in Fig. 2.

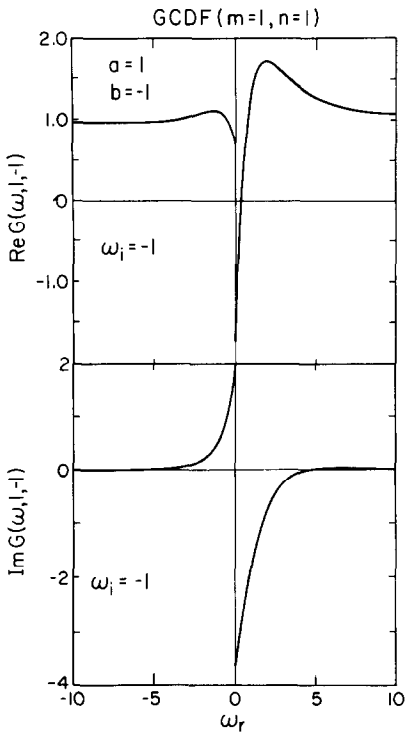

FIG. 7. Graph of the real and imaginary parts of $G(\omega, a = 1, b = -1)$ for $\omega_i = -1$. The discontinuity at $\omega_r = 0$ arises from the branch line shown in Fig. 2.

REFERENCES

1. C. W. HORTON, J. D. CALLEN, AND M. N. ROSENBLUTH, *Phys. Fluids* **14** (1971), 2019.
2. T. M. ANTONSEN AND B. LANE, *Phys. Fluids* **23** (1980), 1205.
3. B. D. FRIED AND S. D. CONTE, "The Plasma Dispersion Function," Academic Press, New York, 1961.
4. P. W. TERRY, W. C. ANDERSON, AND W. HORTON, *Nucl. Fusion* **22** (1982), 487.
5. H. L. BERK, J. W. VAN DAM, AND M. N. ROSENBLUTH, *Phys. Fluids* **26** (1983), 526.